Physica B ■ (■■■■) ■■■–■■■

Contents lists available at ScienceDirect

Physica B

journal homepage: www.elsevier.com/locate/physb

Co-Dopant Influence on the Persistent Luminescence of $BaAl_2O_4:Eu^{2+},R^{3+}$

Lucas C.V. Rodrigues [a,b,*], Jorma Hölsä [a,b,c], José M. Carvalho [b], Cássio C.S. Pedroso [b], Mika Lastusaari [a,c], Maria C.F.C. Felinto [d], Shigeo Watanabe [e], Hermi F. Brito [b]

[a] University of Turku, Department of Chemistry, FI-20014 Turku, Finland
[b] Universidade de São Paulo, Instituto de Química, Av. Prof. Lineu Prestes 748, 05508-000 São Paulo-SP, Brazil
[c] Turku University Centre for Materials and Surfaces (MatSurf), Turku, Finland
[d] Instituto de Pesquisas Energéticas e Nucleares, Centro de Química e Meio Ambiente, Av. Prof. Lineu Prestes 2242, 05508-000 São Paulo-SP, Brazil
[e] Universidade de São Paulo, Instituto de Física, Rua do Matão, Travessa R 187, 05508-090 São Paulo-SP, Brazil

ARTICLE INFO

Keywords:
Persistent luminescence
Defects
Thermoluminescence
XANES
$BaAl_2O_4$
Rare Earth

ABSTRACT

The R^{3+} (rare earth) co-dopants may have a surprisingly important role in persistent luminescence – enhancement of up to 1–3 orders of magnitude may be obtained in the performance of these phosphor materials – depending strongly on the R^{3+} ion, of course. In this work, the effects of the R^{3+} co-dopants in the $BaAl_2O_4:Eu^{2+},R^{3+}$ materials were studied using mainly thermoluminescence (TL) and synchrotron radiation XANES methods. In $BaAl_2O_4$, the conventional and persistent luminescence both arise from the $4f^7 \rightarrow 4f^65d^1$ transition of Eu^{2+}, yielding blue–green emission color. The former, in the presence of humidity, turns to more bluish because of creation of an additional Eu^{2+} luminescence centre which is not, however, visible in persistent luminescence. The trap structure in the non-co-doped $BaAl_2O_4:Eu^{2+}$ is rather complex with 4–5 TL bands above room temperature. With R^{3+} co-doping, this basic structure is modified though no drastic change can be observed. This underlines the fact that even very small changes in the trap depths can produce significant modifications in the persistent luminescence efficiency. It should be remembered that basically the persistent luminescence performance is controlled by the Boltzmann population law depending exponentially on both the temperature and trap depth.

Some mechanisms for persistent luminescence have suggested the presence of either divalent R^{2+} or tetravalent R^{IV} during the charging of the Eu^{2+} doped materials. The present XANES measurements on $BaAl_2O_4:Eu^{2+},R^{3+}$ confirmed the presence of only the trivalent form of the R^{3+} co-dopants excluding both of these pathways. It must thus be concluded, that the energy is stored in intrinsic and extrinsic defects created by the synthesis conditions and charge compensation due to R^{3+} co-doping. Even though the effect of the R^{3+} co-dopants was carefully exploited and characterized, the differences in the effect of different R^{3+} ions with very similar chemical and spectroscopic properties could not be explained in a satisfactory manner. More work is – and perhaps a completely new approach may be – needed.

1. Introduction

In persistent luminescence, which is nominally an isothermal case of thermally stimulated luminescence, the material continues to emit light for several hours after ceasing the irradiation [1,2]. These materials can be applied in emergency signalization, micro defect sensing, optoelectronics for image storage, detectors of high energy radiation, thermal sensors, *in vivo* imaging, *etc.* [1–3]. The recent progress in the research of persistent luminescence materials is related to the discovery of the $SrAl_2O_4:Eu^{2+},Dy^{3+}$ phosphor [2] in 1996. The initial innovation was soon followed by a family of new efficient persistent luminescence materials based mainly on different aluminates and silicates with higher chemical stability, *e.g.* $CaAl_2O_4:Eu^{2+},Nd^{3+}$ [1], $Sr_4Al_{14}O_{25}:Eu^{2+},Dy^{3+}$ [4] and $Sr_2MgSi_2O_7:Eu^{2+},Dy^{3+}$ [5]. Presently, the best materials can continue to emit light in excess of 24 h in the dark. Among the aluminate materials, $BaAl_2O_4:Eu^{2+},R^{3+}$ have a special advantage that europium can be reduced and kept in the divalent state without the use of any reducing atmosphere [6–8] which facilitates the preparation of these persistent luminescence materials.

According to the present understanding, in persistent luminescence the excitation energy is stored to traps and then released with the stimulation by thermal energy available at room temperature [1]. In most – if not in all – Eu^{2+} doped persistent luminescence materials the traps' properties can be modified by

* Corresponding author at: Universidade de São Paulo, Instituto de Química, Av. Prof. Lineu Prestes 748, 05508-000 São Paulo-SP, Brazil. Tel.: +55 11 30913708; fax: +55 11 3815 5640.
E-mail address: lucascvr@iq.usp.br (L.C.V. Rodrigues).

0921-4526/$ - see front matter © 2013 Elsevier B.V. All rights reserved.
http://dx.doi.org/10.1016/j.physb.2013.11.007

using different trivalent rare earth (R^{3+}) co-dopants [1,9]. In order to improve the intensity and duration of the persistent luminescence, it is important to know genuinely the role of the R^{3+} co-dopants in the mechanism of the phenomenon, not just to note that this happened to be the outcome of co-doping. The genuine knowledge is very important to reduce the amount of human and financial resources dedicated to the development of new materials. This work was thus aimed to study the role of the R^{3+} co-dopants in modifying the trap structure in $BaAl_2O_4:Eu^{2+},R^{3+}$ and how these modifications affect the efficiency of persistent luminescence.

2. Experimental

2.1. Materials preparation

The $BaAl_2O_4:Eu^{2+},R^{3+}$ materials were prepared using the combustion synthesis route starting with the metal nitrates and urea as the reactants and the fuel, respectively. The rare earth nitrate hydrates were obtained from the respective rare earth oxides (R_2O_3, Pr_6O_{11} or Tb_4O_7; 99.99% CSTARM) or from $Ce_2(CO_3)_3$ (99.99% Aldrich) with a reaction with concentrated nitric acid. The precursors were then dissolved into a smallest possible amount of distilled water. A silica capsule filled with the homogeneous solution was inserted into a furnace pre-heated to 500 °C [6,10–12]. The reaction began *ca.* 5 min after the introduction of the capsule into the furnace. The mixture was then self-ignited with a white flame and produced a white powder. After the completion of the reaction, the furnace was turned off and allowed to cool freely. The products were removed from the oven when the temperature had decreased to *ca.* 25 °C. The nominal concentrations of Eu^{2+} and R^{3+} were 1 and 2 mol-% (of the Ba^{2+} amount), respectively. The formation of Eu^{2+} using Eu^{3+} as a source without the use of reducing atmosphere has been explained to result from the evaporation of the interstitial oxygen at high temperatures [6].

2.2. Methods of characterization

The crystal structure and phase purity of the $BaAl_2O_4:Eu^{2+},R^{3+}$ materials were routinely verified with the X-ray powder diffraction measurements using a Rigaku Miniflex diffractometer with $CuK_{\alpha 1}$ radiation (1.5406 Å) between 3 and 90° (in 2θ) with 0.02° and 1 s as the 2θ step and step time, respectively.

The luminescence spectra and persistent luminescence decay times were measured with a SPEX Fluorolog-2 spectrofluorometer equipped with two 0.22 m SPEX 1680 double grating monochromators. A 450 W Xenon lamp was used as the excitation and irradiation source. The CIE color coordinates were calculated based on the emission spectra using the SpectraLux v2.0 software [13].

The thermoluminescence (TL) glow curves of the $BaAl_2O_4:Eu^{2+},R^{3+}$ phosphors were recorded with a Daybreak TL Reader 1100 thermoluminescence system with a linear heating rate of 5 °C s^{-1} in the temperature range between 25 and 400 °C. The global TL emission from UV to 650 nm was monitored using the bialkali EMI 9235QA photomultiplier and the Corning 7-59 and Schott BG-39 filters. Prior to the TL measurements, the materials were exposed to radiation from a 6 W Cole-Parmer UV lamp (emission maxima at 254 and 365 nm). Exposure and delay times were 2 and 3 min, respectively. The analysis of the TL glow curves was carried out by deconvoluting the TL curves with the program TLanal v.1.0.3 [14,15]. The fitted bands were considered to be of either the 1st or 2nd order kinetics depending on the asymmetry of the band profile.

The X-ray Absorption Near-Edge Structure (XANES) measurements of the rare earth elements in $BaAl_2O_4:Eu^{2+},R^{3+}$ persistent luminescence materials were carried out at room temperature using the beamline I811 at MAX-lab in Lund, Sweden [16]. The data were collected in the fluorescence mode over the rare earth L_{II} and L_{III} edges using the Si(111) double crystal monochromator with a 7 element Gresham Si(Li) detector. The energy resolution $\Delta E/E$ was 10^{-4} and the measured energy range was from 100 eV both before and after the edge.

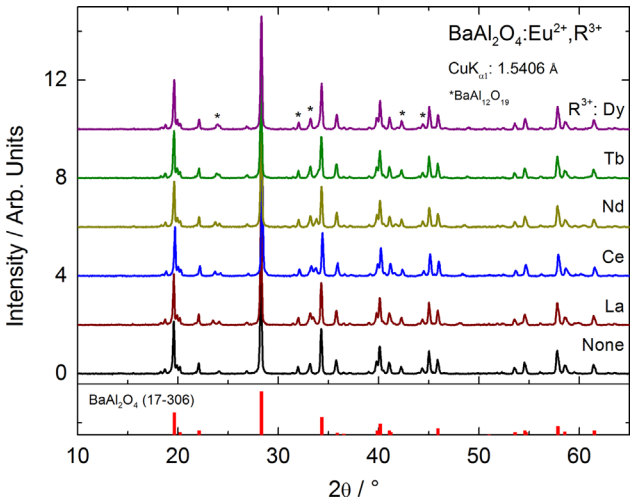

Fig. 1. X-Ray diffraction patterns of the $BaAl_2O_4:Eu^{2+},R^{3+}$ materials.

3. Results and discussion

3.1. Formation and phase purity

The X-ray diffraction patterns (Fig. 1) confirm the formation of the hexagonal $BaAl_2O_4$ phase though usually with a small amount of $BaAl_{12}O_{19}$ as a sole impurity phase [17]. The presence of this impurity is mainly due to the high temperature achieved locally and for a short period of time during the combustion synthesis; estimates range from up to at least 1600 °C [18] but, depending on the fuel and oxidizer, temperatures as high as 3000 °C may be achieved. The local temperature may clearly exceed that required for the formation of $BaAl_2O_4$, as low as 1300 °C. No significant differences were observed in either the 2θ positions or FWHM values of the XRD reflections between materials with different co-dopants, most probably due to the low dopant concentrations used.

3.2. Photoluminescence of $BaAl_2O_4:Eu^{2+},R^{3+}$

The UV excited luminescence spectra of $BaAl_2O_4:Eu^{2+},R^{3+}$ confirm the role of Eu^{2+} as the emitting ion, since only the broad $4f^65d^1 \rightarrow 4f^7$ emission bands are observed with the maxima at 430 and 500 nm (Fig. 2), yielding a bluish-green emission with the CIE color coordinates x, y of 0.128, 0.414 (Fig. 2, inset). The emission spectra of the materials with different co-dopants are very similar, irrespective of the R^{3+} co-dopant, in agreement with previous work [19]. The 430 nm band arises from the creation of a new Eu^{2+} site due to water exposure [20,21]. Since this band is not observed in the persistent luminescence spectrum of *e.g.* the Dy^{3+} co-doped material, it may be due to a new compound rather than a modification of the existing $BaAl_2O_4$.

Despite the close similarity of the emission spectra, the persistent luminescence decay times are strongly influenced by the co-dopant. The materials with Dy^{3+} and Nd^{3+} as the co-dopant show the longest duration of persistent luminescence, followed by

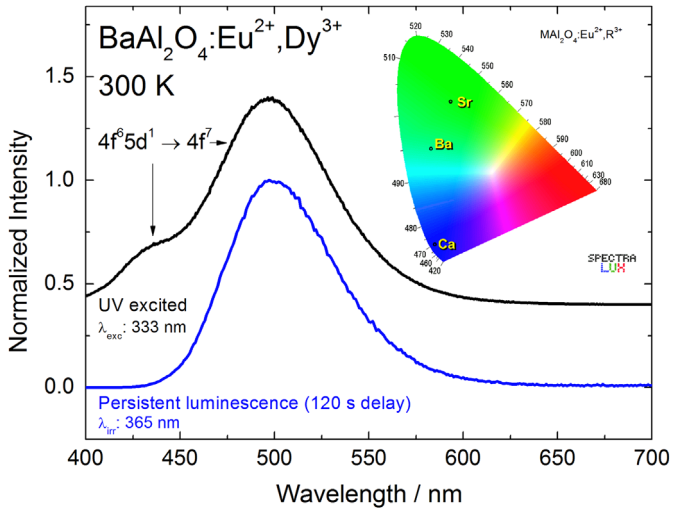

Fig. 2. UV excited and persistent luminescence spectra of $BaAl_2O_4:Eu^{2+},Dy^{3+}$. The inset reproduces the CIE color coordinates of persistent luminescence from $MAl_2O_4:Eu^{2+},R^{3+}$ (M: Ca, Sr and Ba) in the color diagram.

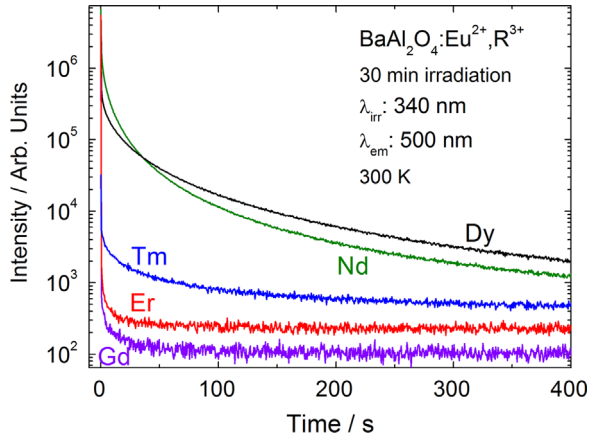

Fig. 3. The persistent luminescence decay curves of selected $BaAl_2O_4:Eu^{2+},R^{3+}$.

Tm^{3+} and then Er^{3+} (Fig. 3). The other co-dopants, *e.g.* Gd^{3+}, yield very short persistent luminescence observed only with difficulty by a human eye.

3.3. *Trap depths in $BaAl_2O_4:Eu^{2+},R^{3+}$*

The different mechanisms developed for the persistent luminescence phenomenon [1,9,22,23], despite some differences, agree on that prior to the persistent emission, the irradiation energy is stored in defects in the material. Even though the nature of the defects (hole or electron traps) is not yet known in detail, their essential properties as the number, depth, and density can be studied with different methods. Since the persistent emission can be considered as an isothermal case of thermally stimulated luminescence, the thermoluminescence (TL) methods have proven to be the most suitable ones to probe the trap properties. However, information concerning neither the nature nor origin of the traps is easily obtained from the TL glow curves [24,25].

For the $BaAl_2O_4:Eu^{2+},R^{3+}$ system, the TL glow curves of the materials co-doped with La^{3+}, Ce^{3+}, Sm^{3+}, Gd^{3+} and Tb^{3+} are characterized by lower than or very similar intensity as the non-co-doped material (Fig. 4, top). Due to the low concentration of defects in these materials, no visible persistent luminescence can be observed or detected at room temperature after ceasing the irradiation. On the other hand, the Pr^{3+}, Nd^{3+}, Dy^{3+}, Er^{3+} and

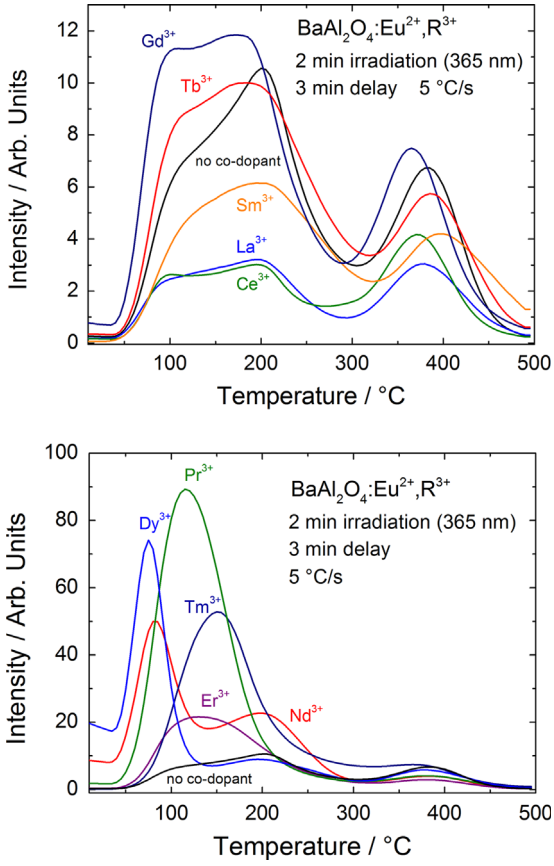

Fig. 4. Thermoluminescence glow curves of $BaAl_2O_4:Eu^{2+},R^{3+}$ (R: none, La, Ce, Sm, Gd and Tb (top) and none, Pr, Nd, Dy, Er and Tm (bottom)).

Tm^{3+} co-dopants yield higher TL intensity than the material without a co-dopant (Fig. 4, bottom). The co-dopants Nd^{3+} and Dy^{3+} possess high trap concentration combined with a close to ideal temperature maximum (*ca.* 75 °C) and, consequently, these materials have the longest persistent luminescence decay times (Fig. 3) at room temperature. Despite the high trap concentration of the materials co-doped with Pr^{3+}, Er^{3+} and Tm^{3+}, the maxima of the TL glow curves are located above 100 °C, too high a temperature for efficient persistent luminescence to be operational at room temperature. These results indicate that materials with the Pr^{3+}, Er^{3+} and Tm^{3+} co-dopants could be used for high temperature applications. The very short persistent luminescence decay times presented by these materials, however, suggest that, in addition to the high temperature traps, there are also very low energy ones that are bleached too fast at the room temperature. These very shallow traps are not detected by the conventional thermoluminescence technique used and low temperature measurements must thus be done in the future to clarify the present predictions.

As a result of a detailed analysis of the TL curves by using the deconvolution method [14,15], a good agreement between the experimental and calculated glow curves was obtained by using five traps with depths between 0.82 and 1.44 eV as shown for the Dy^{3+} co-doped material (Fig. 5). The non-co-doped materials or co-doped with different R^{3+} also present 4 to 5 traps with energy ranging from 0.8 to 1.45 eV. In the deconvolution process, all bands were considered to follow the second order kinetics, indicating efficient retrapping which is an important information when constructing the mechanism for persistent luminescence.

The presence of defects in the non-co-doped material can have different origins. The first one is the evaporation of BaO due to

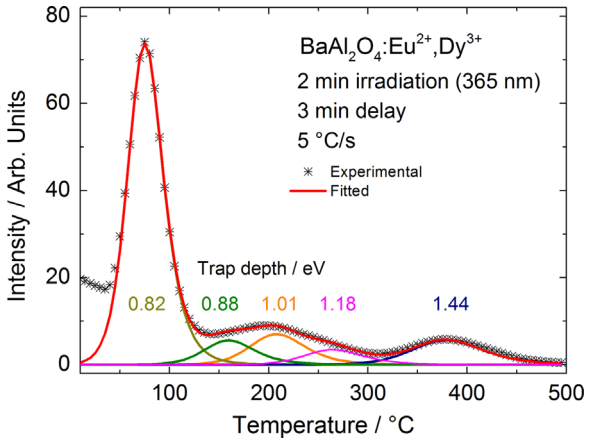

Fig. 5. Deconvolution of the TL glow curve of $BaAl_2O_4:Eu^{2+},Dy^{3+}$.

the high temperatures achieved locally during the combustion reaction, forming barium and oxide vacancies, exemplified as V''_{Ba} and $V^{\bullet\bullet}_{O}$ by using the Kröger–Vink notation [26]. The existence of intrinsic defects cannot be ruled out though their concentration should not be significant at room temperature. However, if the defects were frozen into the lattice after the rather rapid quenching from the high preparation temperature, the situation is much different. The presence of such defects was, moreover, confirmed with theoretical DFT calculations [20] which displayed non-negligible density of states close to the bottom of the conduction band (CB) of the non-doped $BaAl_2O_4$. Finally, since it is almost impossible to reduce all Eu^{3+} to Eu^{2+}, the trivalent form can also act as a R^{3+} co-dopant and cause defects due to charge compensation.

The co-doping of $BaAl_2O_4$ with R^{3+} generates charge compensation defects related to the presence of R^{3+} in the Ba^{2+} sites, the aliovalent substitution requiring the creation of either interstitial oxide ions or Ba^{2+} vacancies as follows:

$$2Ba^{x}_{Ba} \rightarrow 2R^{\bullet}_{Ba} + O''_{i} \quad (1)$$

$$2Ba^{x}_{Ba} \rightarrow 2R^{\bullet}_{Ba} + V''_{Ba} \quad (2)$$

The interstitial oxide might have reduced stability due to increased oxygen–oxygen repulsion as observed in the $CdSiO_3$ case [27]. The O''_i may then be replaced by electrons and these trapped species can have an important role to play in the storage of energy for persistent luminescence. Furthermore, the mechanism of the spontaneous reduction of Eu^{3+} to Eu^{2+} without the use of a reducing atmosphere, suggested that, for the $BaAl_2O_4$ material, this involves the release of the interstitial oxides as oxygen [6]. Therefore, the reduced stability of O''_i may be related to this reduction, but further studies with other hosts should be carried out combining simultaneously experimental data with theoretical calculations using *e.g.* the DFT methods.

3.4. Valence of the R^{3+} co-dopant

The mechanism of the Eu^{2+} persistent luminescence assumes that electrons from the excited Eu^{2+} ion migrate to the host's CB and then to traps. This may be interpreted as photoionization of the Eu^{2+} ion to become trivalent Eu^{3+} [28], though the presence of such a species has not been shown unequivocally by X-ray absorption near edge spectroscopy (XANES) measurements. Inconclusive results are to be expected since the X-ray beam may cause the oxidation of Eu^{2+} to Eu^{3+} [6,29] especially with extended exposure times. The presence of a Eu^{3+} signal in the XANES spectra may thus be an experimental artifact. The role of the co-dopant in the persistent luminescence mechanism is still uncertain, as well. One of the suggested mechanisms [23] assumes that the R^{3+} co-dopant traps an electron, to form R^{2+}, though, once again, there is no evidence of the presence of the R^{2+} ions in $BaAl_2O_4:Eu^{2+},R^{3+}$. It should be relatively easy to detect the different species by XANES since the white lines of rare earth ions with different valence are typically separated by *ca.* 8 eV in the spectra. The present rare earth L_{II} or L_{III} edge data for the $BaAl_2O_4:Eu^{2+},R^{3+}$ materials (Fig. 6) show the presence of only the trivalent form, suggesting that if the co-dopants act as electron traps, R^{3+}–e^- pairs instead of the R^{2+} species will be created.

3.5. Persistent luminescence mechanism

The information about the trap depths and the valence of the co-dopant yielded important data to support and complement the current knowledge [6,30] on the mechanism (Fig. 7) of persistent luminescence from $BaAl_2O_4:Eu^{2+},R^{3+}$. The complete process can be split into two parts which may be quite independent from each other – though sharing some of the contributors as the Eu^{2+} dopant: (1) the charging – *i.e.* energy storage, and (2) the decharging, *i.e.* the actual persistent luminescence. The former partial mechanism considers for $BaAl_2O_4:Eu^{2+},R^{3+}$ that: (i) under irradiation with energies above 2.6 eV (*i.e.* the energy of the $4f^7 \rightarrow 4f^6 5d^1$ transition of Eu^{2+}), in addition to the conventional Eu^{2+} luminescence, some electrons escape to the $BaAl_2O_4$ CB, forming simultaneously the pair Eu^{2+}–h^+; (ii) after migration in the host's CB, the electrons are trapped from the CB to defects comprising the intrinsic ones and to those created by BaO evaporation and charge compensation due to the aliovalent

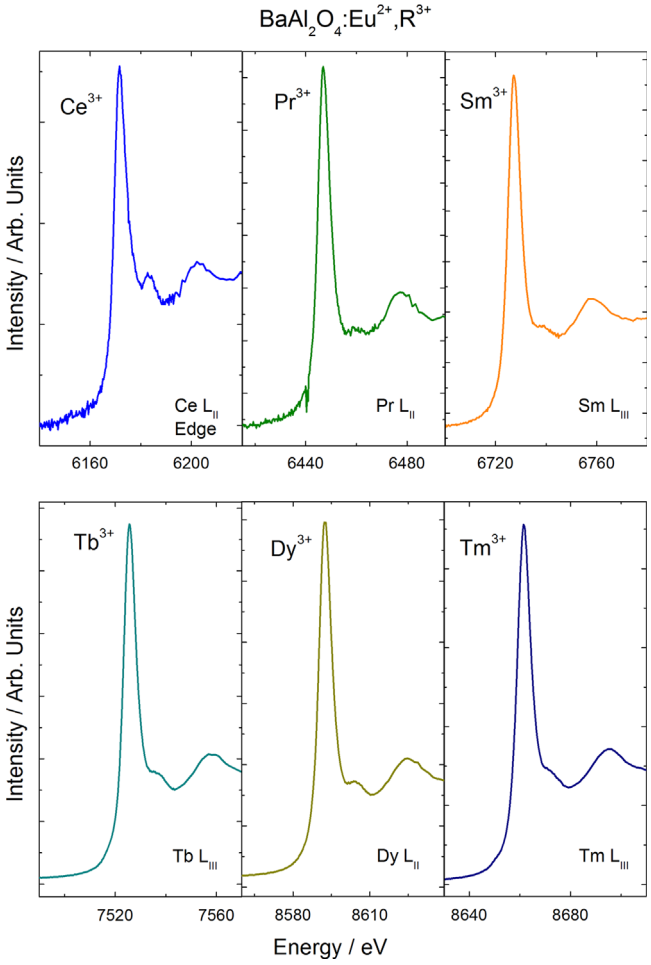

Fig. 6. Synchrotron radiation XANES spectra of selected $BaAl_2O_4:Eu^{2+},R^{3+}$.

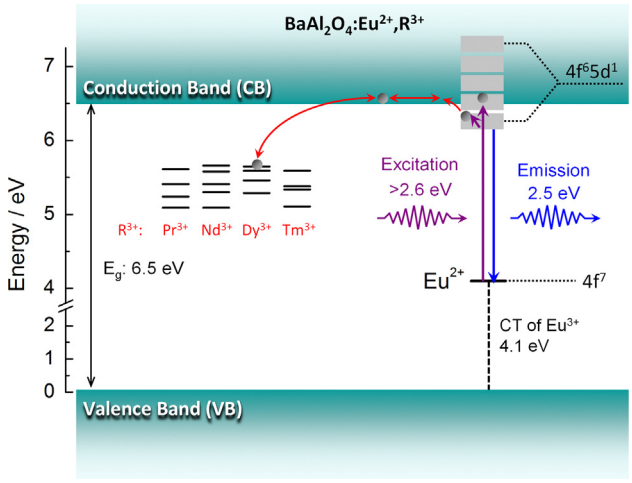

Fig. 7. The persistent luminescence mechanism in $BaAl_2O_4:Eu^{2+},R^{3+}$.

$R^{3+} \rightarrow Ba^{2+}$ substitution. The excitation energy is stored in the traps until the system acquires thermal energy sufficient for the latter reverse decharging process, where the electrons are freed from the traps to the excited states *via* CB, finally returning to the ground state *via* radiative relaxation, creating the persistent luminescence.

4. Conclusions

The $BaAl_2O_4:Eu^{2+},R^{3+}$ materials show identical blue–green persistent luminescence with all the rare earth co-dopants though only Nd^{3+} and Dy^{3+} co-doping yield efficient persistent luminescence at room temperature. On the other hand, Pr^{3+}, Er^{3+} and Tm^{3+} co-doping generate deeper traps, useful for high temperature applications of persistent luminescence. Based on the XANES results, it can be concluded that the absence of the divalent form of the rare earth co-dopants indicates that, if the electrons are trapped by R^{3+}, R^{3+}–e^- pairs are formed instead of R^{2+}. However, more probable trapping sites for electrons are the intrinsic defects as well as those formed by aliovalent substitution of Ba^{2+} by R^{3+}. The deconvolution of the TL glow curves yielded the trap energies, though more detailed studies, *e.g.* TL fading experiments are needed to resolve the overlapping bands. The trap structures resulting from different R^{3+} co-doping are not really different enough to explain the drastic differences in the persistent luminescence performance of the different materials. Of course, the low temperature TL measurements may bring more light to this issue. Eventually, a fine-tuning of the Eu^{2+} persistent luminescence mechanism and the role of defects may also be achieved by simultaneous theoretical studies using *e.g.* the DFT methods.

Acknowledgements

Financial support is acknowledged from the Conselho Nacional de Desenvolvimento Científico e Tecnológico (CNPq, Brazil), Fundação de Amparo à Pesquisa do Estado de São Paulo (FAPESP, Brazil), Instituto Nacional de Ciência e Tecnologia de Nanotecnologia para Marcadores Integrados (inct-INAMI, Brazil), Coordenação de Aperfeiçoamento de Pessoal de Nível Superior (CAPES, Brazil), Academy of Finland (contract #137333/2010) and Coimbra Group (LCVR). The synchrotron research leading to these results has also received funding from the European Community's Seventh Framework Programme (FP7/2007-2013) under grant agreement n° 226716. Dr. Stefan Carlson and Dr. Katarina Norén (beam line I811, MAX-lab, Lund Sweden) are gratefully acknowledged for their assistance during the synchrotron measurements. The authors also thank Dr. Roseli Gennari, Ms Adriana Alves and Ms Débora Gonçalves (Universidade de São Paulo, Instituto de Física) for the thermoluminescence measurements.

References

[1] T. Aitasalo, J. Hölsä, H. Jungner, M. Lastusaari, J. Niittykoski, J. Phys. Chem. B 110 (2006) 4589.
[2] T. Matsuzawa, Y. Aoki, N. Takeuchi, Y. Murayama, J. Electrochem. Soc. 143 (1996) 2670.
[3] T. Maldiney, A. Lecointre, B. Viana, A. Bessière, M. Bessodes, D. Gourier, C. Richard, D. Scherman, J. Am. Chem. Soc. 133 (2011) 11810.
[4] Y. Lin, Z. Tang, Z. Zhang, C.W. Nan, Appl. Phys. Lett. 81 (2002) 996.
[5] Y. Lin, Z. Tang, Z. Zhang, X. Wang, J. Zhang, J. Mater. Sci. Lett. 20 (2001) 1505.
[6] L.C.V. Rodrigues, R. Stefani, H.F. Brito, M.C.F.C. Felinto, J. Hölsä, M. Lastusaari, T. Laamanen, M. Malkamäki, J. Solid State Chem. 183 (2010) 2365.
[7] R. Stefani, L.C.V. Rodrigues, C.A.A. Carvalho, M.C.F.C. Felinto, H.F. Brito, M. Lastusaari, J. Hölsä, Opt. Mater. 31 (2009) 1815.
[8] M. Peng, G. Hong, J. Lumin. 127 (2007) 735.
[9] K. Van den Eeckhout, P.F. Smet, D. Poelman, Materials 3 (2010) 2536.
[10] Z. Qiu, Y. Zhou, M. Lu, A. Zhang, Q. Ma, Acta Mater. 55 (2007) 2615.
[11] S. Ekambaram, K.C. Patil, M. Maaza, J. Alloys Compd. 393 (2005) 81.
[12] B.M. Mothudi, O.M. Ntwaeaborwa, J.R. Botha, H.C. Swart, Physica B 404 (2009) 4440.
[13] P.A. Santa-Cruz, F.S. Teles, SpectraLux Software v. 2.0, Ponto Quântico Nanodispositivos/RENAMI, Recife-PE Brazil, 2003.
[14] K.S. Chung, H.S. Choe, J.I. Lee, J.L. Kim, S.Y. Chang, Radiat. Prot. Dosim. 115 (2005) 345.
[15] K.S. Chung, TL Glow Curve Analyzer v.1.0.3, Korea Atomic Energy Research Institute and Gyeongsang National University, Korea, 2008.
[16] S. Carlson, M. Clausen, L. Gridneva, B. Sommarin, C. Svensson, J. Synchrotron Rad. 13 (2006) 359.
[17] The International Centre for Diffraction Data – ICDD, Powder Diffraction File, Entries 17-306 ($BaAl_2O_4$) and 26-0135 ($BaAl_{12}O_{19}$), 1997.
[18] H.S. Jeon, S.K. Kim, H.L. Park, G.C. Kim, J.H. Bang, M. Lee, Solid State Commun. 120 (2001) 221.
[19] M.A. Lephoto, O.M. Ntwaeaborwa, S.S. Pitale, H.C. Swart, J.R. Botha, B. M. Mothudi, Physica B 407 (2012) 1603.
[20] H.F. Brito, M.C.F.C. Felinto, J. Hölsä, T. Laamanen, M. Lastusaari, M. Malkamäki, P. Novák, L.C.V. Rodrigues, R. Stefani, Opt. Mater. Express 2 (2012) 420.
[21] A.V.S. Lourenço, L.C.V. Rodrigues, C.A. Kodaira, R. Stefani, H.F. Brito, M.C.F.C. Felinto, J. Hölsä, 11th International Conference on Advanced Materials, September 20–25, Rio de Janeiro-RJ, Brazil, BB556 ⟨http://www.sbpmat.org.br/icam2009/pdf/BB556.pdf⟩, 2009.
[22] F. Clabau, X. Rocquefelte, T. Le Mercier, P. Deniard, S. Jobic, M.H. Whangbo, Chem. Mater. 18 (2006) 3212.
[23] P. Dorenbos, Phys. Status Solidi B 242 (2005) R7.
[24] J. Trojan-Piegza, J. Niittykoski, J. Hölsä, E. Zych, Chem. Mater. 20 (2008) 2252.
[25] R. Chen, S.W.S. McKeever, Theory of Thermoluminescence and Related Phenomena, World Scientific, Singapore, 1997.
[26] F.A. Kröger, H.J. Vink, in: Proceedings of the International Colloquium, Garmisch-Partenkirchen, Germany, 1958, p. 17.
[27] L.C.V. Rodrigues, H.F. Brito, J. Hölsä, R. Stefani, M.C.F.C. Felinto, M. Lastusaari, T. Laamanen, L.A.O. Nunes, J. Phys. Chem. C 116 (2012) 11232.
[28] K. Korthout, K. Van den Eeckhout, J. Botterman, S. Nikitenko, D. Poelman, P.F. Smet, Phys. Rev. B 84 (2011) 085140.
[29] J. Hölsä, T. Laamanen, M. Lastusaari, M. Malkamäki, E. Welter, D.A. Zajac, Spectrochim. Acta B 65 (2010) 301.
[30] L.C.V. Rodrigues, H.F. Brito, J. Hölsä, M. Lastusaari, Opt. Mater. Express 2 (2012) 382.